

## Plasmon enhancement of photosensitivity of Ag–chalcogenide glass thin film structures

I.Z. Indutnyi, S.V. Mamykin, V.I. Mynko, M.V. Sopinsky, A.A. Korchovyi

V. Lashkaryov Institute of Semiconductor Physics, National Academy of Sciences of Ukraine,  
41, prospect Nauky, 03680 Kyiv, Ukraine  
E-mail: i.indutnyi@gmail.com; indutnyi@isp.kiev.ua

**Abstract.** In this paper, we present the results of studying the features of plasmon-enhanced photostimulated diffusion of silver into thin films of chalcogenide glasses (ChG), in particular,  $\text{As}_2\text{S}_3$  and  $\text{GeSe}_2$ . To ensure excitation of surface plasmon-polaritons (SPPs) at the interface between silver and ChG films, silver diffraction gratings with periods of 899 and 694 nm were used as substrates. The samples were exposed to the  $p$ -polarized radiation of a He-Ne laser ( $\lambda = 632.8$  nm). The radiation of the same laser, attenuated by two orders of magnitude, was used to detect SPP, which enabled to study the kinetics of photostimulated processes in the thin-layer structure of Ag–ChG. It has been established that in the initial period of exposure, the SPP electromagnetic field significantly enhances the photostimulated flux of silver ions in ChG (by 2-3 times). The photodissolution kinetics of Ag in ChG is defined by the features of the granular structure of the investigated thin chalcogenide films. For the  $\text{GeSe}_2$  film with the effective thickness 8 nm, the kinetics of the film refractive index increase caused by silver photodoping is well approximated by a logarithmic dependence. For the Ag– $\text{As}_2\text{S}_3$  structure (the effective thickness of the  $\text{As}_2\text{S}_3$  film is 14.8 nm), this kinetics is closer to the linear one; moreover, for photodoping without SPP excitation, the kinetics is somewhat superlinear, while with plasmon excitation, it is sublinear. The main physical mechanism responsible for the acceleration of the process of photostimulated diffusion in the structure under study appears to be an accelerated generation of electron-hole pairs, which takes place in the ChG layer near the interface with the metal, where the SPP electromagnetic field strength is maximum, and/or plasmon-assisted hot carrier generation due to plasmon scattering on the surface of the metal film and subsequent internal photoemission of electrons from silver into chalcogenide.

**Keywords:** surface plasmon polariton, photostimulated diffusion, chalcogenide glass, Ag.

<https://doi.org/10.15407/spqeo26.04.432>

PACS 71.36.+c, 73.20.Mf, 77.84.Bw, 78.20.-e

Manuscript received 08.09.23; revised version received 25.09.23; accepted for publication 22.11.23; published online 05.12.23.

### 1. Introduction

Photostimulated dissolution of silver in thin layers of chalcogenide glasses (ChG) leads to significant changes in both the optical characteristics of these layers and the rate of their dissolution in selective etchants. The phenomenon of photodissolution (the terms “photodissolution”, “photodoping”, “photostimulated diffusion” are used in the literature as synonyms) is observed when light, electron or ion beams are falling onto a thin-layer structure consisting of films of amorphous chalcogenide glass ( $\text{As}_2\text{S}_3$ ,  $\text{GeSe}_2$ , etc.) and silver. This phenomenon, discovered more than half a century ago [1], serves as the basis for the use of thin layer photosensitive Ag–ChG structures in photolithography, optoelectronics,

for recording information, including for nonvolatile memory devices, in photoelectric devices, etc. [2–7]. As a result of studying the mechanism of light-stimulated processes in thin-layer Ag–ChG structures [8–11], it was found that at the first stage of silver photodissolution, the defining factor is absorption of light at the interface between ChG and Ag; therefore, the intensity of photostimulated silver diffusion depends on the light intensity in the region of this interface.

In recent years, the attention of researchers has been attracted by the possibility to increase the photosensitivity of these structures due to excitation of surface plasmon-polaritons (SPPs) at the interface between silver and ChG layers, when the Ag–ChG structure is exposed [12–14]. SPPs are characterized by the localization of the

electromagnetic field near the metal-dielectric interface, where the strength of the electromagnetic field significantly exceeds the one of the exciting radiation. Such a local amplification of the electro-magnetic field near a metal film or nanostructure due to excitation of the SPP has found wide practical application in various sensors [15–17]. In previous works [12–14], it was found that at the initial stage of the photodoping process in the Ag–ChG structure, an increase in the diffusion flux of silver into the chalcogenide layer is observed, when a surface plasmon-polariton is excited at the silver-chalcogenide interface during exposure. This indicates acceleration of the process of photostimulated diffusion in these structures under the action of a plasmon field. These results were obtained on the most studied structures based on  $\text{As}_2\text{S}_3$  [12, 13], as well as on the basis of  $\text{As}_4\text{Ge}_{30}\text{S}_{66}$  triple glasses. However, the recent studies [6, 7] have shown that the most promising chalcogenides for use in non-volatile memory devices and photovoltaic installations are germanium chalcogenides. In addition, they are more environmentally compatible than arsenic chalcogenides. Therefore, this paper presents the results of comparative studies of the features inherent to the plasmon enhancement of photostimulated diffusion of silver in ChGs of two compositions  $\text{As}_2\text{S}_3$  and  $\text{GeSe}_2$ .

## 2. Experimental

To provide SPP excitation, diffraction gratings on polished glass plates, fabricated by interference lithography based on vacuum chalcogenide photoresists, were used as sample substrates. The technique for manufacturing these gratings is described in detail in our previous papers [3, 18]. The resulting gratings formed on a film of  $\text{As}_2\text{S}_2\text{Se}$  chalcogenide photoresist thermally deposited in vacuum were covered with the 80-nm thick Al layer, on which an opaque 85-nm thick silver layer was deposited (both of these layers were also deposited by thermal evaporation in vacuum). The thickness of the silver film was chosen in such a way as to prevent SPP excitation at the lower boundary of the Ag layer. The aluminum layer was deposited to prevent diffusion of silver into the bottom layer of the chalcogenide photoresist. The gratings had spatial periods  $a = 899$  and  $694$  nm, as well as relief depths  $h = 95$  and  $28$  nm, respectively, which ensured sufficient SPP excitation efficiency, when the structure is exposed at the resonant angle of incidence [14]. Then layers of chalcogenide  $\text{As}_2\text{S}_3$  or  $\text{GeSe}_2$  with the thickness close to  $14.8$  and  $8$  nm, respectively, were thermally deposited on silver in vacuum. In this case, the vacuum chamber and the obtained light-sensitive samples were shielded from external illumination. Thermal evaporation of the chalcogenides (the  $\text{As}_2\text{S}_2\text{Se}$  photoresist and thin  $\text{As}_2\text{S}_3$  and  $\text{GeSe}_2$  films) was carried out using a labyrinth-type molybdenum evaporator, making it possible to reproduce the ChG stoichiometry in the deposited films with the accuracy of approximately 1 at. %.

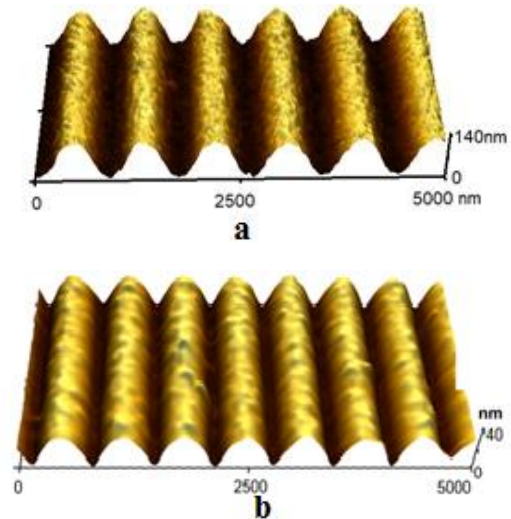


**Fig. 1.** AFM images of the gratings with the periods 899 nm (a) and 694 nm (b).

The thickness of the layers was controlled during deposition using a KIT-1 graduated quartz thickness gauge, and for thin layers of chalcogenides it was also measured after deposition using a LEF3-M-1 laser ellipsometer. To record the grating relief and study the structure of reference samples of the  $\text{As}_2\text{S}_3$  and  $\text{GeSe}_2$  thin films, we used a Dimension 3000 scanning probe microscope (Digital Instruments Inc., Tonawanda, New York, USA). Since the depth of the grating relief in our case was significantly less than their periods ( $h/a \leq 12\%$ ), the thin layers of Al, Ag, and ChG deposited on its surface (as shown by AFM studies) almost did not distort the profile of these “shallow” grooves inherent to the original substrates. Fig. 1 shows an AFM image of the grating relief with the periods 899 nm (a) and 694 nm (b). The shown images were obtained after depositing the aluminum layer onto the corresponding chalcogenide gratings. The cross-sectional shape of the surface typical to the grooves of this gratings is somewhat different from the sinusoidal one (slightly expanded peaks and narrowed troughs), which is due to the characteristics of the chalcogenide photoresist (the degree of linearity of its characteristic curve) and the technological mode of sample preparation [19].

To observe photostimulated diffusion of silver in the investigated Ag–ChG structures, they were exposed from chalcogenide side by the  $p$ -polarized radiation of a He-Ne laser ( $\lambda = 632.8$  nm). The power density of the light incident on the sample upon exposure was  $32 \text{ mW/cm}^2$ . As it is known [8–11], the photosensitivity spectrum of these structures mainly correlates with the absorption spectrum of the corresponding chalcogenide. Therefore, the  $\text{As}_2\text{S}_3$ –Ag and  $\text{GeSe}_2$ –Ag structures are weakly sensitive to radiation of this wavelength, which corresponds to the spectral region of the Urbach absorption of these glasses. This enables to study in sufficient detail the initial stage of photodoping in our

samples. The grating with the deposited structure was fixed on a rotating table of a stand mounted on the basis of a G5M goniometer and a Microscope Universal Stage (LOMO 5-axis Universal Fedorov Stage). The angle of incidence  $\theta$  of the laser beam could be varied within  $0...90^\circ$  with the accuracy  $0.01^\circ$  (the angle of incidence is defined as the angle between the laser beam incident on the grating and the normal to the sample surface), and the azimuth angle  $\varphi$  (the angle between the plane of incidence and the reciprocal grating vector) – within the same limits with the accuracy  $0.1^\circ$ . In these studies, the sample was oriented in such a way that the grating grooves were perpendicular to the plane of incidence of the exposing radiation ( $\varphi = 0$ ).

To control the photostimulated changes in the Ag–ChG structures as a result of exposure, we also used registration of SPP. These studies were carried out on the same test bench by measuring the specular reflection of  $p$ -polarized radiation from the same laser. In this case, the intensity of the laser beam was attenuated by two orders of magnitude by using neutral grey filters in order to reduce the effect of the probing beam on the light-sensitive structure under study. The plane of incidence of the probing beam was the same as that for the exposure radiation. The laser radiation passed through the first polarizer, was reflected from the grating, and, after passing through the second polarizer, hit the photodiode. Separating the  $p$ -component in the reflected light with the second polarizer and comparing it with the incident polarized radiation, we obtain the angular dependences of the absolute value of the  $p$ -component specular reflection coefficient ( $R_p$ ).

### 3. Results and discussion

The light-sensitive ChG–Ag structures studied in this work contain an “excessive” thickness silver layer and much thinner layers of  $\text{As}_2\text{S}_3$  and  $\text{GeSe}_2$ . The term “excessive” is understood to mean such an amount of silver that clearly cannot be photo-dissolved in the used thin ChG layers. In addition, thin ChG layers with a thickness of 5 to 20 nm thermally deposited in vacuum can have a granular structure, which will significantly affect their optical characteristics. Therefore, reference samples of thin  $\text{As}_2\text{S}_3$  and  $\text{GeSe}_2$  layers on the silicon substrates were prepared using simultaneous deposition of these ChGs on the silver gratings and silicon substrates. AFM and ellipsometric studies were performed on the control samples to determine morphology and the effective thickness of these layers.

Fig. 2a shows an AFM image of the relief of reference  $\text{As}_2\text{S}_3$  layer obtained using a probe with a tip radius of 7 nm. It can be seen that the film has a granular structure; the distribution histograms of granule diameters and relief heights are shown in Figs 2b and 2c. Relief heights are measured relatively to the minimum height value on the sample area under study  $1000 \times 1000$  nm.

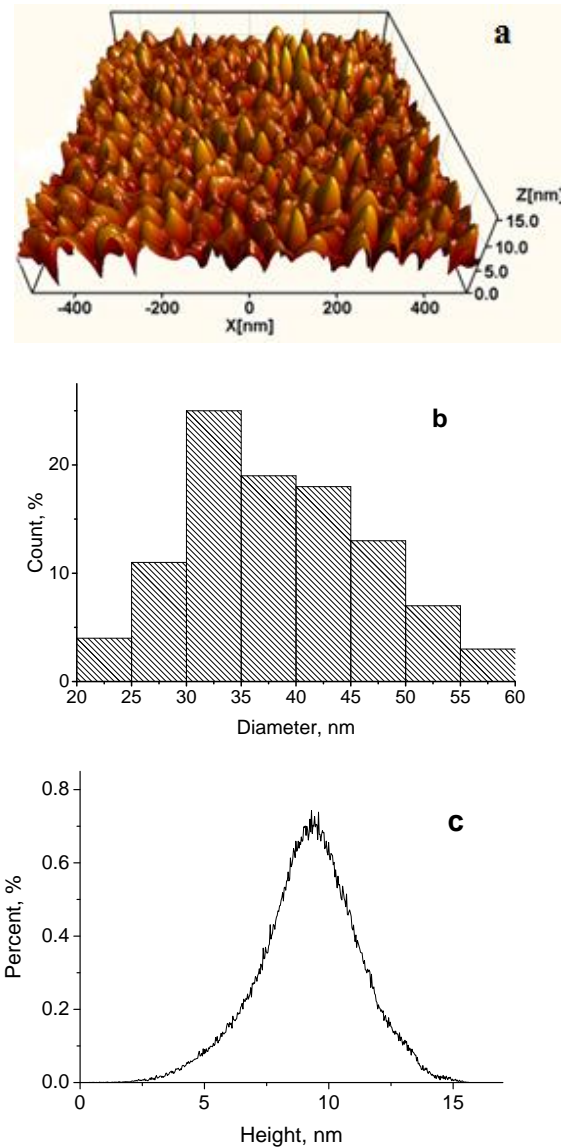


**Fig. 2.** AFM image (a) and distribution histograms of granule diameters (b) and relief heights (c) of thin  $\text{As}_2\text{S}_3$  layer deposited onto a silicon substrate.

Similar results were also obtained for the reference  $\text{GeSe}_2$  layer (not shown). The film also has a granular structure, but the granule diameters and relief heights are much smaller than those for the  $\text{As}_2\text{S}_3$  layer. Thus, for the reference  $\text{As}_2\text{S}_3$  layer, the granule diameters vary from 20 up to 60 nm, and the maximum of the distribution histograms of granule diameters corresponds to the size range of 30...35 nm. In the same film, the relief heights vary from 0 to 15 nm, and the maximum of the distribution histogram corresponds to the height of 9.5 nm. For the  $\text{GeSe}_2$  film, the granule size range is from 4 to 22 nm (the histogram maximum corresponds to the diameter range of 7 to 9 nm); the heights of the relief vary from 0 to 4 nm, with a distribution maximum at 1.4 nm. This difference in the structure of the films may be caused by the conditions of their deposition. It is

known that the granularity of a thermally deposited film is related with the ratio  $T_s/T_m$ , where  $T_s$  is the substrate temperature and  $T_m$  is the melting temperature of bulk material [20]. The smaller the ratio, the more fine-grained the film structure is. In our case, the melting temperature of GeSe<sub>2</sub> is much higher (by almost 200 °C) than that of As<sub>2</sub>S<sub>3</sub> at almost identical substrate temperatures. This will favor formation of larger granules during deposition of As<sub>2</sub>S<sub>3</sub>. In addition, the size of the granules may depend on the thickness of film. In a thinner GeSe<sub>2</sub> film, smaller granules can be formed.

Ellipsometric multi-angle measurements enabled to determine the effective thickness  $d_f$  and refractive index  $n_f$  of these granular films. The values  $d_f = 14.8$  nm,  $n_f = 2.16$  for the As<sub>2</sub>S<sub>3</sub> film, and  $d_f = 8.0$  nm,  $n_f = 2.09$  for the GeSe<sub>2</sub> film were obtained.

When the plane of incidence of the laser beam is oriented along the normal to the grooves of the metal grating, the condition for excitation of the SPP at the boundary of the grating with a dielectric medium is to ensure the conservation of the quasi-momentum, taking into account the wave vector of SPP ( $k_{SPP}$ ), the component of the light's wave vector ( $k_0 = 2\pi/\lambda$ ,  $\lambda$  is the wavelength of the probing radiation), parallel to the grating surface, and the grating vector ( $G = 2\pi/a$ ):

$$\text{Re}(k_{SPP}) = |nk_0 \sin \theta + mG|, \quad (1)$$

where  $m$  is an integer ( $m \neq 0$ ) and means a plasmon resonance order,  $n$  is the refractive index of the environment (for air  $n = 1$ ). In this work, we limited ourselves to studying the effect of only first-order plasmon resonances ( $m = 1$ ) on photostimulated diffusion. By solving equation (1) with respect to  $\theta$  for the chosen wavelength of the exciting radiation, the grating period, and the given permittivities of the metal (silver) and the medium (air), one can determine the resonant angle of incidence  $\theta_r$ , at which SPP excitation is observed. At a fixed excitation wavelength, the plasmon resonance can be observed as a narrow minimum in the angular dependence of the specular reflection ( $R_p$ ) of  $p$ -polarized excitation radiation. Since gratings with a small modulation depth are used in this work, for an approximate estimate of the magnitude of SPP wave vector, we used the expression obtained for the flat interface of semi-infinite media. The value of the permittivity for Ag was taken from [21] ( $\varepsilon = -18.28 + i \cdot 0.481$ ). The calculated values of  $\theta_r$  for the gratings under study when being excited using He-Ne laser radiation with  $\lambda = 632.8$  nm ( $\theta_r = 18.9^\circ$  for a period  $a = 899$  nm and  $6.28^\circ$  for  $a = 694$  nm) correspond to the excitation of SPPs in these gratings with an extremely shallow depth relief. As shown in many theoretical and experimental studies [22], with an increase in the depth of the grating relief, the value of  $\theta_r$  also slightly increases (for an excitation wavelength smaller than the grating period, as in our cases), in addition, the plasmon resonance range expands. When weakly absorbing dielectric films are deposited on these gratings, the resonance is also shifted to larger angles,

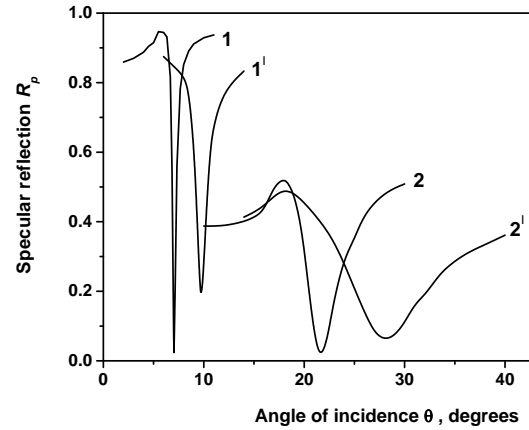


**Fig. 3.** Dependence of specular reflection  $R_p$  on the angle of incidence  $\theta$  for silver-coated grating with the period 694 nm before (1) and after (1') deposition of the 8.0-nm thick GeSe<sub>2</sub> layer; the same for the silver-coated grating with the period 899 nm before (2) and after (2') deposition of the 14.8-nm thick As<sub>2</sub>S<sub>3</sub> layer. The probing wavelength  $\lambda = 632.8$  nm.

and its half-width also increases. The magnitude of this shift is defined mainly by the optical density of the deposited film, *i.e.*, the product of the film thickness and its refractive index.

Fig. 3 shows the angular dependences of the specular reflection of  $p$ -polarized light from the studied silver gratings (curves 1 and 2), as well as for these samples after deposition of thin ChG layers (curves 1' and 2'). The curves 1 and 2 show rather narrow reflection minima associated with SPP excitation, which position corresponds to the resonant angles  $\theta_r = 7.04^\circ$  and  $21.6^\circ$ . After depositing the GeSe<sub>2</sub> and As<sub>2</sub>S<sub>3</sub> layers, the resonance minimum  $R_p$  is shifted towards large angles (up to  $\theta_r = 9.76^\circ$  and  $28.2^\circ$ , accordingly). In addition, the minima of  $R_p$  widen. A slight decrease in the depth of  $R_p$  minima as a result of deposition of thin ChG layers, which is observed in Fig. 3, is a consequence of the small absorption of these layers at the probing wavelength.

The fabricated structures 'Ag grating – thin ChG layer' were used to study the effect of SPP excitation on the photostimulated diffusion of silver into chalcogenide. To do this, identical sections of the sample were exposed to an unattenuated He-Ne laser beam from the side of the chalcogenide layer in two ways: at an angle of incidence normal to the sample surface (in this case, SPP was not excited) and at a resonant angle of incidence  $\theta_r$ , which corresponds to the SPP excitation condition for this sample. As a result of exposure in both cases, photostimulated doping of ChG films with silver occurs, which leads to a change in their optical characteristics, namely: the refractive index and absorption coefficient [9, 11]. To quantitatively register these changes, we used the measurement of the angular dependences of  $R_p$  for the exposed samples and analyzed the changes in the characteristics of plasmon resonances (in particular, the position and depth of the  $R_p$  minimum and its half-width) as a result of exposing. As shown in previous studies

[12–14], this method of recording photostimulated changes in Ag–ChG structures is more sensitive than traditional photometric methods, especially at the initial stages of the process and in thin-layer structures. To study the kinetics of photostimulated changes, the exposure was carried out intermittently: after a certain time, the exposure was turned off and the angular dependence of  $R_p$  was measured with an attenuated beam, then the exposure was continued at the same point of the sample and the angular dependence of  $R_p$  was recorded again. The process was repeated as many times as necessary. For the samples that were exposed with SPP excitation, after each exposure, the angle of exposure was changed, in accordance with the shift of the  $R_p$  minimum.

Figs 4a and 4b show the angular dependence of  $R_p$  for the samples ‘Ag grating – GeSe<sub>2</sub> film’ and ‘Ag grating – As<sub>2</sub>S<sub>3</sub> film’, exposed at resonance angles ( $\theta_{exp} = 9.7\dots10.3^\circ$  for the 8-nm-thick GeSe<sub>2</sub> and  $28.3\dots30.54^\circ$  for the 14.8-nm-thick As<sub>2</sub>S<sub>3</sub> layer). The similar measurements were made with the samples exposed to the laser beam oriented along the normal to the sample surface ( $\theta_{exp} = 0^\circ$ ); *i.e.*, when SPP was not excited during exposure (not shown). For both exposure directions, as well as for both structures, there is a shift ( $\Delta\theta_r$ ) in the position of the  $R_p$  minimum in the direction to larger angles of incidence, simultaneously with expansion (increase in the half-width,  $\Delta\theta_{1/2}$ ) and decrease in the  $R_p$  minimum depth ( $\Delta R_p^{min}$ ). It is known that the indicated characteristics of the plasmon resonance of the ‘metal grating – thin dielectric layer’ structure for a given metal are mainly defined by the characteristics of the dielectric film [22]:  $\Delta\theta_r$  depends on  $n_f d_f$ ;  $\Delta\theta_{1/2}$  is defined by both  $n_f d_f$  and the presence of absorption in the dielectric layer;  $\Delta R_p^{min}$  depends on the absorption in the deposited layer, and/or the roughness of the Ag–film interface. This means that as a result of photodoping in the studied GeSe<sub>2</sub> and As<sub>2</sub>S<sub>3</sub> films with silver, their optical thickness and absorption increase in the region of the light wavelength of 632.8 nm, which is consistent with preliminary studies of photostimulated diffusion in these structures [6, 11, 23].

However, for our samples exposed with SPP excitation, a more significant increase in all three characteristics of the plasmon resonance is observed, as compared to the samples exposed along the normal to the sample surface. It indicates that photostimulated silver doping of ChG films occurs more effectively, when the structure is irradiated together with SPP excitation, especially in the initial period of irradiation. To obtain quantitative characteristics of this process, let us estimate the changes in the optical characteristics of ChG films as a result of photodoping, in particular, changes in the refractive index. We begin by analyzing the morphology of these thin films. As it follows from the analysis of results obtained in AFM investigations, the studied GeSe<sub>2</sub> and As<sub>2</sub>S<sub>3</sub> films are granular, and their optical characteristics can be described using the Bruggemann effective medium model. Before photodoping with silver,

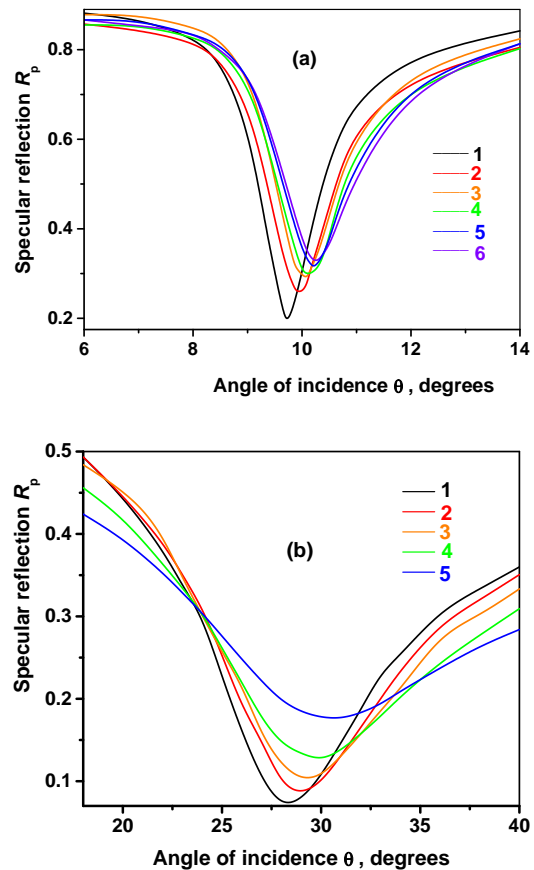


**Fig. 4.** Angular dependences of specular reflection  $R_p$  for the ‘Ag grating – 8-nm-thick GeSe<sub>2</sub> layer’ (a) and ‘Ag grating – 14.8-nm-thick As<sub>2</sub>S<sub>3</sub> layer’ (b) structures exposed at resonance angles. Exposure and measurement wavelength  $\lambda = 632.8$  nm. Exposure time (min) in Fig. 4a: 0 (1), 0.5 (2), 1.5 (3), 3.5 (4), 7.5 (5), 11.5 (6); in Fig. 4b: 0 (1), 1.0 (2), 2.33 (3), 3.67 (4), 6.33 (5).

they have a two-phase structure (ChG and air) with a significant air content (porosity,  $p_f$ ). This is also evidenced by the above effective values of  $n_f$  for deposited films (2.16 for As<sub>2</sub>S<sub>3</sub> and 2.09 for GeSe<sub>2</sub>), which are much smaller than the literature data and the results of our measurements [24–26] for thicker non-porous layers and glasses (2.66 for GeSe<sub>2</sub> and 2.46 for As<sub>2</sub>S<sub>3</sub>). Using these results, it is possible to estimate the porosity of the studied ChG films after deposition by applying the Bruggeman model. We obtain the values  $p_f = 0.35$  for GeSe<sub>2</sub> and 0.21 for As<sub>2</sub>S<sub>3</sub>. This significant porosity values allow us to fairly reasonably neglect the possible change in the effective thickness of the ChG film upon photodoping with silver, in subsequent estimates of the change in the refractive index, since expansion of chalcogenide matrix upon photodoping with silver will be damped due to the ‘collapse’ of the voids.

Thus, assuming  $d_f$  to be a constant, we use the approximate formula proposed by Homola [27] to estimate the change in the effective refractive index of SPP ( $N_{SPP} = \text{Re}(k_{SPP})/k_0$ ) as a result of deposition of a thin

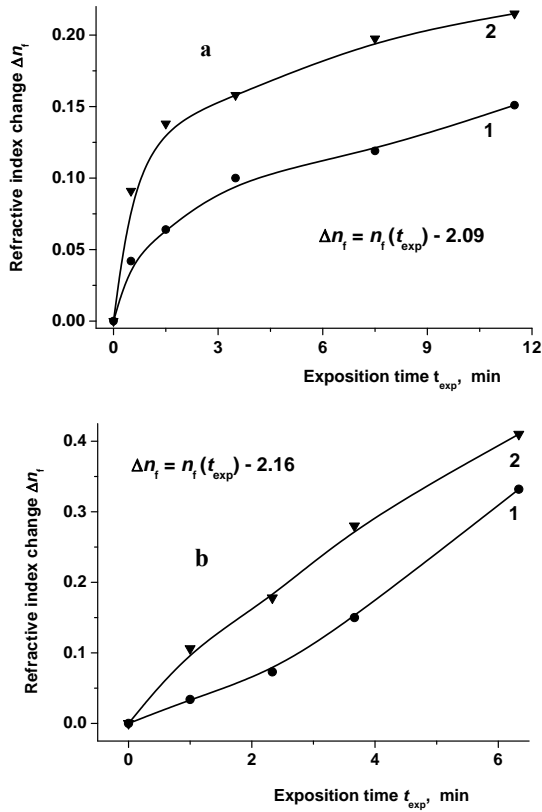


**Fig. 5.** Kinetics of the increase in the effective refractive index ( $\Delta n_f = n_f(t_{exp}) - n_f(t_{exp} = 0)$ ) during photodoping with silver of the  $\text{GeSe}_2$  (a) and  $\text{As}_2\text{S}_3$  (b) layers for the exposure at  $\theta_{exp} = 0^\circ$  (1) and  $\theta_{exp} = \theta_{res}$  (2).

dielectric layer of thickness  $d_f$  with a refractive index  $n_f$  on the grating surface:

$$\Delta N_{SPP} = \frac{2d_f}{l_d} \frac{N_{SPP}^3}{n^3} \Delta n, \quad (2)$$

where  $\Delta n = n_f - n$ ,  $n$  is the refractive index of the medium (in our case for air  $n = 1$ ). Using the equations (1) and (2), as well as the experimental values of  $\Delta\theta_r$ , we calculated the average values of  $n_f$  for the both photodoped chalcogenide films.

Fig. 5 shows the obtained kinetics of the growth of the effective refractive index of the studied granular  $\text{GeSe}_2$  (5a) and  $\text{As}_2\text{S}_3$  (5b) films upon photodoping with silver. The samples were exposed both perpendicular to the sample surface ( $\theta_{exp} = 0^\circ$ ), that is, without excitation of SPP (curves 1), and at resonant angles corresponding to the excitation of SPP ( $\theta_{exp} = \theta_{res}$ , curves 2).

The more significant increase in  $\Delta n_f$  was observed for both samples upon exposure with SPP excitation, especially in the initial period of irradiation. The maximum ratio of  $\Delta n_f$  for curves 1 and 2  $\Delta n_f(2)/\Delta n_f(1)$  was observed after irradiation for the first exposure interval and was equal to 2.22 and 3.15 for ‘Ag grating –  $\text{GeSe}_2$ ’ and ‘Ag grating –  $\text{As}_2\text{S}_3$ ’ structures, accordingly. Since SPP ‘degraded’ upon further irradiation, the plasmon field strength continued to decrease. Consequently,

the growth rates of the effective refractive index became comparable for both directions of irradiation, as can be seen from the almost identical behavior of curves 1 and 2 during the third and fourth exposure intervals.

The kinetics of the photostimulated process observed in our samples (Fig. 5) differs significantly from the traditional sigmoidal kinetics of photodoping in ChG–Ag structures [9, 11]. The main feature of the obtained kinetics is the absence of the initial, the so-called ‘‘induction’’ period of a very slow process of formation of the silver diffusion front in the ChG layers. Apparently, this is caused by the granular structure of these thin films. All traditional studies of photodoping in ChG–Ag structures were carried out on much thicker, continuous films of chalcogenides. In our case, the films have a granular structure, and the presence of gaps between the granules can contribute to the rapid surface diffusion of silver into the ChG layer during the initial exposure period for both samples. With further irradiation, the kinetics for ‘Ag grating –  $\text{GeSe}_2$ ’ and ‘Ag grating –  $\text{As}_2\text{S}_3$ ’ structures begin to differ. For the ‘Ag grating –  $\text{As}_2\text{S}_3$ ’ sample, the  $n_f$  growth kinetics are closer to linear, and for photodoping without SPP excitation, the kinetics is somewhat superlinear, and with plasmon excitation, it is somewhat sublinear.

However, for the structure ‘Ag grating –  $\text{GeSe}_2$ ’ neither a linear nor a parabolic dependence describes the obtained experimental points on the kinetic dependence of  $\Delta n_f$ . This kinetics is well approximated by a logarithmic dependence (Fig. 6). Direct and inverse logarithmic kinetics has been reported for oxidation of some metals in the intermediate temperature range (30...300°C), and most generally for relatively small oxide thickness (< 50 nm). This kinetics is also typical to porous films, in which the rapid deceleration of the oxidation rate is caused by an increase in their density during growth [28], that is, due to the ‘‘slamming’’ of pores. As it follows from the results of our AFM studies, for  $\text{GeSe}_2$  films the sizes of granules (and, accordingly, the spaces between them) are 3-4 times smaller than those for  $\text{As}_2\text{S}_3$ . Therefore, for the structures ‘Ag grating –  $\text{GeSe}_2$  film’

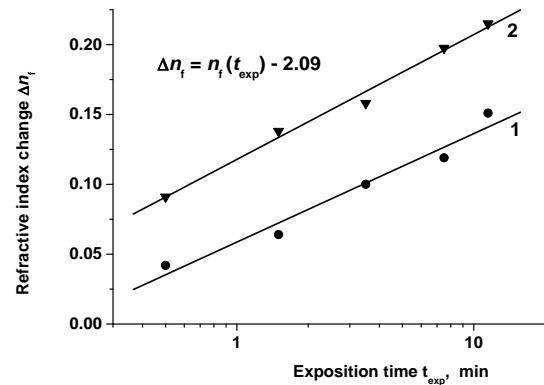


**Fig. 6.** Kinetics of the increase in the effective refractive index ( $\Delta n_f = n_f(t_{exp}) - n_f(t_{exp} = 0)$ ) during photodoping with silver of the  $\text{GeSe}_2$  layers in semi-log coordinates for the exposure at  $\theta_{exp} = 0^\circ$  (1) and  $\theta_{exp} = \theta_{res}$  (2).

**Table 1.** Characteristics of the 8.0-nm thick GeSe<sub>2</sub> film photodoped with silver: refractive index ( $n_f$ ) of the film, value of  $x$  in Ag <sub>$x$</sub> GeSe<sub>2</sub> matrix, atomic concentration of Ag ( $C$ ), refractive index of Ag <sub>$x$</sub> GeSe<sub>2</sub> matrix ( $n_x$ ), porosity of the film ( $p_f$ ).

Exposure angle	Exposure time, min	$n_f$	$x$	$C$ (at.%)	$n_x$	$p_f$
–	0	2.09	0	0	2.66	0.347
normal	0.5	2.13	0.06	1.9	2.72	0.340
normal	1.5	2.15	0.09	2.9	2.74	0.336
normal	3.5	2.19	0.14	4.5	2.78	0.330
normal	7.5	2.21	0.17	5.2	2.80	0.327
normal	11.5	2.24	0.21	6.5	2.83	0.322
resonance	0.5	2.18	0.13	4.1	2.77	0.332
resonance	1.5	2.23	0.19	6.0	2.82	0.324
resonance	3.5	2.25	0.22	6.8	2.84	0.321
resonance	7.5	2.29	0.27	8.3	2.88	0.314
resonance	11.5	2.31	0.29	8.9	2.90	0.312

**Table 2.** Characteristics of the 14.8-nm thick As<sub>2</sub>S<sub>3</sub> film photodoped with silver: refractive index ( $n_f$ ) of the film, value of  $x$  in Ag <sub>$x$</sub> As<sub>2</sub>S<sub>3</sub> matrix, atomic concentration of Ag ( $C$ ), refractive index of Ag <sub>$x$</sub> As<sub>2</sub>S<sub>3</sub> matrix ( $n_x$ ), porosity of the film ( $p_f$ ).

Exposure angle	Exposure time, min	$n_f$	$x$	$C$ (at.%)	$n_x$	$p_f$
–	0	2.16	0	0	2.46	0.211
normal	1.0	2.19	0.10	1.9	2.50	0.203
normal	2.33	2.23	0.21	4.0	2.53	0.194
normal	3.67	2.31	0.42	7.7	2.59	0.177
normal	6.33	2.49	0.90	15.2	2.73	0.139
resonance	1.0	2.27	0.30	5.6	2.56	0.187
resonance	2.33	2.34	0.49	9.0	2.61	0.171
resonance	3.67	2.44	0.76	13.2	2.69	0.149
resonance	6.33	2.57	1.09	17.9	2.79	0.123

the effect of “collapse” of pores appears at lower concentrations of photodoped silver, *i.e.*, at shorter exposures than those for Ag–As<sub>2</sub>S<sub>3</sub>. This, apparently, leads to the logarithmic kinetics of the photodoping process for the structures based on GeSe<sub>2</sub>.

The thin granular silver photodoped ChG films studied in this work can be represented as a two-phase nanocomposite consisting of an Ag <sub>$x$</sub> ChG matrix and air-filled pores. During photodoping, an increase in the atomic content of silver ( $x$ ) in the matrix, some expansion of the matrix (and a corresponding decrease in porosity of the sample  $p_f$ ) occur. It results in an increase in the refractive index of the doped matrix ( $n_x$ ) and the refractive index of the porous composite film ( $n_f$ ). We ascertained the dependence of  $n_f$  on the exposure value for our samples experimentally. To evaluate the remaining characteristics of the studied nanocomposites, we used the literature data on the results of previous studies of GeSe<sub>2</sub> and As<sub>2</sub>S<sub>3</sub> layers photodoped with silver [29, 26]. It turned out that the dependence of  $n_x$  on  $x$  for these compositions is best approximated by straight lines:  $n_x(x) = 2.671 + 0.768x$  for Ag <sub>$x$</sub> GeSe<sub>2</sub> films and  $n_x(x) = 2.470 + 0.293x$  for Ag <sub>$x$</sub> As<sub>2</sub>S<sub>3</sub> films. The second empirical

relationship we used: the thickness of the photodoped pore-free film up to a few percent is equal to the sum of the thicknesses of the components (Ag and ChG). This dependence, taking into account the densities of the components, connects  $x$  and  $p_f$ . In addition, the Bruggemann effective medium model relates  $n_f$ ,  $n_x$ , and  $p_f$ . By solving numerically this system of three equations in three unknowns, we determined the values of  $x$ ,  $p_f$ ,  $n_x$ , as well as the atomic concentration of Ag ( $C$ ) in photodoped GeSe<sub>2</sub> film (Table 1) and As<sub>2</sub>S<sub>3</sub> film (Table 2).

For the first sample (Ag–GeSe<sub>2</sub>) during the initial 30 s of exposure with SPP excitation, 2.2 times more silver is photodissolved in the GeSe<sub>2</sub> layer than that during the same exposure time without SPP, in accord with the data from Table 1. For the Ag–As<sub>2</sub>S<sub>3</sub> structure, this difference after the first minute of exposure is 2.9 times (Table 2). Thus, SPP excitation during photodoping leads to a significant increase in the photo-stimulated flux of Ag into the ChG layer in the initial exposure period. The maximum obtained value of silver content in our samples is 8.9 at.% for the GeSe<sub>2</sub> layer and 17.9 at.% for the As<sub>2</sub>S<sub>3</sub> layer. This is much less than the maximum concentration values obtained in previous

studies for thick layers: 33 at.% for GeSe<sub>2</sub> [30] and 41 at.% for As<sub>2</sub>S<sub>3</sub> [11]. That is, in our study, we register mainly the initial stage of the photodoping process in ChG–Ag structures.

The main physical mechanism responsible for acceleration of the process of photostimulated diffusion in the structure under study seems to be the accelerated generation of electron-hole pairs, which occurs in the ChG layer near the interface with the metal, where the intensity of the SPP electromagnetic field has its maximum. Another possible mechanism for the generation of carriers that stimulate the photoenhanced diffusion of Ag ions during SPP excitation can be plasmon-assisted generation of hot carriers due to plasmon decay on the surface of the metal film and internal photoemission of electrons from silver into chalcogenide [31, 32]. The emitted electrons are captured by traps in the ChG layer near the interface with the metal. Then, this excitation and relaxation of the electron subsystem in the irradiated structure is accompanied by mass transfer through the Ag–ChG interface due to diffusion and/or drift of silver ions.

#### 4. Conclusions

It has been ascertained that in the initial period of irradiation of the light-sensitive Ag–ChG structure, the electromagnetic field of surface plasmon-polaritons significantly enhances the photostimulated flux of silver ions in ChG (2-3 times). As a result, the photosensitivity of the structures increases: upon irradiation at the angle corresponding to SPP excitation, the photodoping process is completed several times faster. For the GeSe<sub>2</sub> film, the kinetics of  $n_f$  growth due to silver photodoping is well approximated by a logarithmic dependence. But for the As<sub>2</sub>S<sub>3</sub> sample, the  $n_f$  growth kinetics is closer to the linear one, and for photodoping without SPP excitation the kinetics is somewhat superlinear, while with plasmon excitation, it is somewhat sublinear. This difference in kinetics is mainly caused by the difference in the characteristics of the granular structure of thin chalcogenide films.

The concentration of photodissolved silver in chalcogenide layers has been estimated. Possible mechanisms promoting acceleration of photostimulated metal diffusion in the Ag–ChG structure as a result of SPP excitation have been discussed. In particular, an increase in the electromagnetic field strength of the incident radiation near the Ag–ChG interface as a result of SPP excitation, as well as generation of hot carriers due to plasmon scattering on the surface of the metal film, can stimulate an increase in the flux of drifting Ag<sup>+</sup> ions and accelerate photodissolution of silver in ChG.

#### Acknowledgement

This work was partially supported by National Research Foundation of Ukraine (Grant No. 2022.01/0126, “Development and implementation of a dust-insensitive smoke detector based on a plasmon-polariton photodetector”).

#### References

1. Kostyshin M.T., Michailovskaya E.V., Romanenko P.F. On the effect of photographic sensitivity of the thin semiconductor layers deposited on metal substrates. *Sov. Phys. Solid State*. 1966. **8**, No 2. P. 451–452.
2. Murakami Y., Arai K., Wakaki M. *et al.* Application of photo-doping phenomenon in amorphous chalcogenide GeS<sub>2</sub> film to optical device. *Proc. SPIE*. 2015. **9359**. P. 93591N. <https://doi.org/10.1117/12.2078142>.
3. Dan'ko V.A., Indutnyi I.Z., Min'ko V.I., Shepelyavyi P.E. Interference photolithography with the use of resists on the basis of chalcogenide glassy semiconductors. *Optoelectron. Instrument. Proc.* 2010. **46**. P. 483–490. <https://doi.org/10.3103/S8756699011050116>.
4. Kandy A.K., Figueiredo C.S.M., Merino M.F. *et al.* Direct laser writing of computer-generated holograms by photodissolution of silver in arsenic trisulfide. *Optics*. 2023. **4**. P. 138–145. <https://doi.org/10.3390/opt4010010>.
5. Sarwat S.G., Moraitis T., Wright C.D., Bhaskaran H. Chalcogenide optomemristors for multi-factor neuromorphic computation. *Nat. Commun.* 2022. **13**. P. 2247. <https://doi.org/10.1038/s41467-022-29870-9>.
6. Sakaguchi Y., Hanashima T., Simon A.A.A., Mitkova M. Silver photodiffusion into amorphous Ge chalcogenides. Excitation photon energy dependence of the kinetics probed by neutron reflectivity. *Eur. Phys. J. Appl. Phys.* 2020. **90**. P. 30101. <https://doi.org/10.1051/epjap/2020190368>.
7. Smiles M.J., Shalvey T.P., Thomas L. *et al.* GeSe photovoltaics: Doping, interfacial layer and devices. *Faraday Discuss.* 2022. **239**. P. 250–262. <https://doi.org/10.1039/D2FD00048B>.
8. Elliott S.R. A unified mechanism for metal photodissolution in amorphous chalcogenide materials. *J. Non-Cryst. Solids*. 1991. **130**. P. 85–97. [https://doi.org/10.1016/0022-3093\(91\)90159-4](https://doi.org/10.1016/0022-3093(91)90159-4).
9. Stronski A.V. Production of metallic patterns with the help of high resolution inorganic resists. In: Harman G., Mach P. (Eds). *Microelectronic Interconnections and Assembly NATO ASI Series, 3: High Technology*, 54. Springer, Dordrecht, 1998. P. 263–293. [https://doi.org/10.1007/978-94-011-5135-1\\_31](https://doi.org/10.1007/978-94-011-5135-1_31).
10. Priyadarshini P., Das S., Naik R. A review on metal-doped chalcogenide films and their effect on various optoelectronic properties for different applications. *RSC Adv.* 2022. **12**. P. 9599–9620. <https://doi.org/10.1039/D2RA00771A>.
11. Indutnyi I.Z., Kostyshin M.T., Kasiarum O.P. *et al.* *Photostimulated interactions in Metal-Semiconductor Structures*. Kiev, Naukova Dumka, 1992 (in Russian).
12. Indutnyi I.Z., Mynko V.I., Sopinsky N.V., Lytvyn P.M. Plasmon-stimulated photodoping in the thin-layer As<sub>2</sub>S<sub>3</sub>–Ag structure. *Opt. Spectrosc.* 2019. **127**. P. 938–942. <https://doi.org/10.1134/S0030400X19110109>.

13. Indutnyi I., Mynko V., Sopinsky M., Lytvyn P. Impact of surface plasmon polaritons on silver photodiffusion into  $\text{As}_2\text{S}_3$  film. *Plasmonics*. 2021. **16**. P. 181–188. <https://doi.org/10.1007/s11468-020-01275-8>.
14. Indutnyi I.Z., Mynko V.I., Sopinsky M.V. *et al.* The effect of surface plasmon-polaritons on the photostimulated diffusion in light-sensitive  $\text{Ag-As}_4\text{Ge}_{30}\text{S}_{66}$  structures. *SPQEO*. 2021. **24**, No 4. P. 436–443. <https://doi.org/10.15407/spqeo24.04.436>.
15. Toma K., Vala M., Adam P. *et al.* Compact surface plasmon-enhanced fluorescence biochip. *Opt. Exp.* 2013. **21**, No 8. P. 10121–10132. <https://doi.org/10.1364/OE.21.10121>.
16. Valsecchi C., Brolo A.G. Periodic metallic nanostructures as plasmonic chemical sensors. *Langmuir*. 2013. **29**, No 19. P. 5638–5649. <https://doi.org/10.1021/la400085r>.
17. Ding S.Y., Yi J., Li J.F. *et al.* Nanostructure-based plasmon-enhanced Raman spectroscopy for surface analysis of materials. *Nat. Rev. Mater.* 2016. **1**. P. 16021. <https://doi.org/10.1038/natrevmats.2016.21>.
18. Dan'ko V., Dmitruk M., Indutnyi I. *et al.* Fabrication of periodic plasmonic structures using interference lithography and chalcogenide photoresist. *Nanoscale Res. Lett.* 2015. **10**. P. 497. <https://doi.org/10.1186/s11671-015-1203-x>.
19. Indutnyi I.Z., Mynko V.I., Sopinsky M.V. *et al.* Excitation of surface plasmon polaritons on aluminum-coated diffraction gratings formed on an inorganic chalcogenide photoresist: Influence of profile shape. *Plasmonics*. 2022. **17**. P. 2459–2466. <https://doi.org/10.1007/s11468-022-01732-6>.
20. Kaiser N. Review of the fundamentals of thin-film growth. *Appl. Opt.* 2002. **41**, No 16. P. 3053–3060. <https://doi.org/10.1364/AO.41.003053>.
21. Johnson P.B., Christy R.W. Optical constants of the noble metals. *Phys. Rev. B*. 1972. **6**. P. 4370–4379. <https://doi.org/10.1103/PhysRevB.6.4370>.
22. Raether H. *Surface Plasmons on Smooth and Rough Surfaces and on Gratings*. Springer-Verlag Berlin, Heidelberg, 1988.
23. Khan P., Xu Y., Leon W. *et al.* Kinetics of photodissolution within  $\text{Ag/As}_2\text{S}_3$  heterostructure. *J. Non-Cryst. Solids*. 2018. **500**. P. 468–474. <https://doi.org/10.1002/pssa.201870027>.
24. Cazac V., Meshalkin A., Achimova E. *et al.* Surface relief and refractive index gratings patterned in chalcogenide glasses and studied by off-axis digital holography. *Appl. Opt.* 2018. **57**, No 3. P. 507–513. <https://doi.org/10.1364/AO.57.000507>.
25. Yang G., Gueguen Y., Sangleboeuf J.-C. *et al.* Physical properties of the  $\text{Ge}_x\text{Se}_{1-x}$  glasses in the  $0 \leq x \leq 0.42$  range in correlation with their structure. *J. Non-Cryst. Solids*. 2013. **377**. P. 54–59. <http://dx.doi.org/10.1016/j.jnoncrysol.2013.01.049>.
26. Indutnyi I., Mynko V., Sopinsky M., Lytvyn P. Plasmon-enhanced photostimulated diffusion in a thin-layer  $\text{Ag-GeSe}_2$  structure. *J. Non-Cryst. Solids*. 2023. **618**. P. 122513. <https://doi.org/10.1016/j.jnoncrysol.2023.122513>.
27. Homola J. Surface plasmon resonance sensors for detection of chemical and biological species. *Chem. Rev.* 2008. **108**. P. 462–493. <https://doi.org/10.1021/cr068107d>.
28. Zhu Y., Mimura K., Isshiki M. Oxidation mechanism of  $\text{Cu}_2\text{O}$  to  $\text{CuO}$  at 600–1050 °C. *Oxidation of Metals*. 2004. **62**, Nos. 3/4. P. 207–222. <https://doi.org/10.1007/s11085-004-7808-6>.
29. Zekak A. *The Optical Characterisation and Kinetics of Ag Photodissolution in Amorphous As-S Films*. Ph.D. Thesis, University of Edinburgh, Scotland, UK, 1993.
30. Frolet N., Piarristeguy A.A., Ribes M., Pradel A. Morphology and structural studies of Ag photo-diffused  $\text{Ge}_y\text{Se}_{1-y}$  thin films prepared by RF-sputtering. *J. Non-Cryst. Solids*. 2009. **355**, No 37–42. P. 1969–1972. <https://doi.org/10.1016/j.jnoncrysol.2009.05.060>.
31. Brongersma M., Halas N., Nordlander P. Plasmon-induced hot carrier science and technology. *Nature Nanotech.* 2015. **10**. P. 25–34. <https://doi.org/10.1038/nnano.2014.311>.
32. Wu K., Chen J., McBride J.R., Lian T. Efficient hot-electron transfer by a plasmon-induced interfacial charge-transfer transition. *Science*. 2015. **349**(6248). P. 632–635. <https://doi.org/10.1126/science.aac5443>.

#### Authors and CV



**I.Z. Indutnyi**, Doctor of Physics and Mathematics, Professor, Chief Researcher at the V. Lashkaryov Institute of Semiconductor Physics. He is the author of more than 300 publications, including 1 monograph, 35 author's certificates and patents. His main research activity is in the field of optics of thin films,

photostimulated processes in solids and onto surfaces, nanoparticles and nanostructures, interference lithography, plasmonics and sensing.

<https://orcid.org/000-0002-7088-744X>



**S.V. Mamykin**, PhD in Physics and Mathematics, Head of the Department of Polaritonic Optoelectronics and Technology of Nanostructures at the V. Lashkaryov Institute of Semiconductor Physics. He is the author of more than 300 publications. The area of his scientific interests includes optoelectronics, plasmonics, optics, nanophotonics, sensors and photodetectors.

E-mail: [mamykin@isp.kiev.ua](mailto:mamykin@isp.kiev.ua), [smamykin@gmail.com](mailto:smamykin@gmail.com), <https://orcid.org/0000-0002-9427-324X>



**V.I. Mynko**, PhD in Physics and Mathematics, Senior Researcher at the V. Lashkaryov Institute of Semiconductor Physics. He is the author of more than 170 publications, including 1 monograph and 14 author's certificates and patents. Area of interest includes inorganic

resists and their application in lithography, holography, optical engineering and information storage.

E-mail: mynkoviktor@gmail.com,

<https://orcid.org/0000-0001-6307-7054>



**M.V. Sopinsky**, PhD in Physics and Mathematics, Senior Researcher at the V. Lashkaryov Institute of Semiconductor Physics. Authored over 150 publications. The area of his scientific interests includes interference lithography, photo- and thermostimulated processes in thin-film structures, plasmonics, synthesis and characterization of nanomaterials, ellipsometry.

<http://orcid.org/0000-0002-0101-1241>,

E-mails: [sopinsky@ua.fm](mailto:sopinsky@ua.fm), [sopinsky@isp.kiev.ua](mailto:sopinsky@isp.kiev.ua)



**A.A. Korchovi**, PhD in Physics and Mathematics. Senior Researcher at the Laboratory of Electron probe methods for the diagnostics of materials, V. Lashkaryov Institute of Semiconductor Physics. Authored over 80 publications. The area of his research interests includes atomic force microscopy, physical and chemical properties of semiconductors, chemicals and nanostructures for modern micro- and nano-electronics.

E-mail: [akorchovi@gmail.com](mailto:akorchovi@gmail.com),

<https://orcid.org/0000-0002-8848-7049>

#### Authors' contributions

**Indutnyi I.Z.:** conceptualization, methodology, measurements, writing – original draft, writing – review & editing.

**Mamykin S.V.:** conceptualization, methodology, measurements, writing – review & editing.

**Mynko V.I.:** conceptualization, preparation of samples for research.

**Sopinsky M.V.:** conceptualization, measurements, modeling, visualization, writing – review & editing.

**Korchovi A.A.:** measurements, visualization.

### Плазмонне підсилення світлочутливості тонкоплівкових структур Ag–халькогенідне скло

I.Z. Індутний, С.В. Мамікін, В.І. Минько, М.В. Сопінський, А.А. Корчовий

**Анотація.** У даній статті наведено результати дослідження особливостей плазмонного підсилення фотостимульованої дифузії срібла в тонкі півки халькогенідних стекел (ХС), зокрема  $As_2S_3$  та  $GeSe_2$ . Для забезпечення збудження поверхневих плазмон-поляритонів (ППП) на інтерфейсі між сріблом та півками ХС як підкладки використовувались срібні дифракційні ґратки з періодами 899 та 694 нм. Зразки експонувались з боку шару халькогеніду  $p$ -поляризованим випромінюванням He-Ne-лазера ( $\lambda = 632,8$  нм). Випромінювання цього ж лазера, ослаблене на два порядки, використовувалося для реєстрації ППП, що дозволило дослідити кінетику фотостимульованих процесів у тонкошаровій структурі Ag–ХС. З'ясовано, що у початковий період експонування електромагнітне поле ППП суттєво підсилює фотостимульований потік іонів срібла в ХС (у 2-3 рази). Кінетика фоторозчинення Ag у ХС визначається характеристиками гранулярної структури досліджуваних тонких плівок халькогенідів. Для півки  $GeSe_2$  з ефективною товщиною 8 нм кінетика зростання показника заломлення півки внаслідок фотолегвання сріблом добре апроксимується логарифмічною залежністю. Для структури Ag– $As_2S_3$  (ефективна товщина півки становить 14,8 нм) кінетика більш близька до лінійної, причому для фотолегвання без збудження ППП кінетика дещо суперлінійна, а при збудженні плазмона – сублінійна. Основним фізичним механізмом, відповідальним за прискорення процесу фотостимульованої дифузії в досліджуваних структурах, є прискорена генерація електронно-діркових пар, яка відбувається в шарі ХС поблизу межі поділу з металом, де напруженість електромагнітного поля ППП максимальна, та/або генерування гарячих носіїв внаслідок розсіяння плазмону на поверхні металеві півки та подальшої внутрішньої фотоемісії електронів зі срібла в халькогенід.

**Ключові слова:** поверхневий плазмон-поляритон, фотостимульована дифузія, халькогенідне скло, Ag.